Structural Modulation Study of Inhibitory Compounds for Ribonuclease H Activity of Human Immunodeficiency Virus Type 1 Reverse Transcriptase

Hiroshi Yanagita,[a] Satoshi Fudo,[a] Emiko Urano,[b] Reiko Ichikawa,[b] Masakazu Ogata,[a] Mizuho Yokota,[a] Tsutomu Murakami,[b] Honggui Wu,[b,c] Joe Chiba,[c] Jun Komano,[b] and Tyuji Hoshino*[,a]

[a] *Graduate School of Pharmaceutical Sciences, Chiba University; 1–8–1 Inohana, Chuo-ku, Chiba 260–8675, Japan:* [b] *AIDS Research Center, National Institute of Infectious Diseases; 1–23–1 Toyama, Shinjuku-ku, Tokyo 162–8640, Japan: and* [c] *Faculty of Industrial Science and Technology, Tokyo University of Science; 2641 Yamazaki, Noda, Chiba 278–8510, Japan.* Received February 23, 2012; accepted April 4, 2012

Reverse transcriptase of human immunodeficiency virus type 1 (HIV-1) has two enzymatic functions. One of the functions is ribonuclease (RNase) H activity concerning the digestion of only RNA of RNA/DNA hybrid. The RNase H activity is an attractive target for a new class of anti-HIV drugs because no approved inhibitor is available now. In our previous studies, an agent bearing 5-nitro-furan-2-carboxylic acid ester core was found from chemical screening and dozens of the derivatives were synthesized to improve compound potency. In this work, some parts of the chemical structure were modulated to deepen our understanding of the structure–activity relationship of the analogous compounds. Several derivatives having nitro-furan-phenyl-ester skeleton were shown to be potent RNase H inhibitors. Attaching methoxy-carbonyl and methoxy groups to the phenyl ring increased the inhibitory potency. No significant cytotoxicity was observed for these active derivatives. In contrast, the derivatives having nitro-furan-benzyl-ester skeleton showed modest inhibitory activities regardless of attaching diverse kinds of functional groups to the benzyl ring. Both the modulation of the 5-nitro-furan-2-carboxylic moiety and the conversion of the ester linkage resulted in a drastic decrease in inhibitory potency. These findings are informative for designing potent inhibitors of RNase H enzymatic activity of HIV-1.

Key words antiviral drug; ribonuclease H enzymatic activity; nitro-furan-phenyl-ester; human immunodeficiency virus type 1 reverse transcriptase; inhibitor

Human immunodeficiency virus type 1 (HIV-1) reverse transcriptase (RT) is a multi-functional enzyme that facilitates both polymerase and ribonuclease (RNase) H activities and converts the single-stranded viral RNA into a double-stranded DNA. There exist two active sites in HIV-1 RT responsible for the respective enzymatic functions. Currently, two classes of RT inhibitors, nucleoside reverse transcriptase inhibitors (NRTIs) and non-nucleoside reverse transcriptase inhibitors (NNRTIs), are used clinically. The formers compete with the natural deoxyribonucleotide triphosphate (dNTP) for nucleoside incorporation and act as chain terminators after incorporation.[1)] The latter agents are bound to an adjacent location from the polymerase active site and block RT polymerase function.[2)] Both of these inhibitors are targeting polymerase activity of RT. In contrast, no approved inhibitor is available for RNase H activity, although there have been several reports on the inhibitors that target the RNase H activity of HIV-1 RT.[3–5)] The role of RNase H activity in the reverse transcription process is to remove the viral genomic RNA during the synthesis of double-stranded DNA.[6,7)] Agents targeting RNase H function is expected to be complimentary to the currently standard chemotherapy. Hence, RT-associated RNase H activity is one of the attractive targets for developing a novel class of antiviral drugs. Furthermore, the potential for dual inhibition of RNase H activity and integrase activity of HIV-1 has been examined because of the structural similarity of their catalytic sites.[8–10)]

HIV-1 RNase H is known to utilize two divalent metals for catalysis.[11–13)] The RNase H dual metal mechanism was suggested from high resolution co-crystal structures of *Bacillus halodurans* RNase H with RNA/DNA hybrids at different stages along the reaction pathway of phosphodiester cleavage.[14,15)] The active site contains four carboxyl residues, creating an environment capable of holding two metal ions. It has been assumed that many RNase H inhibitors bind to the catalytic center interacting with two divalent metal ions simultaneously.

Diketo acids are known to work as potent inhibitors for divalent metal-related enzymes.[16)] Therefore, diketo acid structure has served as a starting point for the design and optimization of inhibitors of HIV-1 integrase or influenza endonuclease. Pyrimidinol is another typical agent bearing a scaffold called *N*-hydroxyimide.[17)] *N*-Hydroxyimides were firstly described as inhibitors of influenza endonuclease, but they also show a high potency in biochemical assays of HIV-1 RNase H. A natural product β-thujaplicinol is another scaffold and shows a high inhibitory potency for HIV-1 RNase H activity.[18)]

From an *in vitro* screening using 20000 chemical compounds, we found chemicals that blocked HIV-1 RT-associated RNase H activity.[19)] The agents bearing the 5-nitro-furan-2-carboxylic acid ester moiety turned out to work as an RNase H inhibitor. Two of the agents were capable of suppressing HIV-1 replication in tissue culture. On the basis of the hit chemicals found in the screening, more than 50 derivatives of 5-nitro-furan-2-carboxylic acid were synthesized.[20)] Inhibitory potency of RNase H enzymatic activity was measured in a biochemical assay. Several derivatives showed higher

The authors declare no conflict of interest.

* To whom correspondence should be addressed. e-mail: hoshino@chiba-u.jp

inhibitory activities than those of the hit chemicals. Modulation of the 5-nitro-furan-2-carboxylic moiety resulted in a decrease in inhibitory potency. In contrast, many derivatives with modulation of other parts maintained inhibitory activities. These studies indicate that the nitro-furan-carboxylic moiety is one of the potent scaffolds for RNase H inhibitor.

In this study, we further synthesized chemical compounds bearing the 5-nitro-furan-2-carboxylic acid ester moiety and examined the potency for anti-HIV drugs blocking RT-associated RNase H enzymatic activity. The potency of the synthesized compounds was evaluated through the measurement of inhibitory activity with real-time monitoring of fluorescence emission from the digested RNA substrate. In addition, the cytotoxicity of these compounds was assessed in 293T cells. Computer simulation with molecular dynamics (MD) method was also performed to analyze the stability of the binding structure of an active compound.

Experimental

Organic Synthesis Compound **1** was synthesized by creating an ester linkage between a nitro-furan carboxylic acid and an α-chloro-amide bound with benzyl and penthyl groups, by 3 h reaction at 60°C in dimethylformamide (DMF) in the presence of dimethyl-aminopyridine (DMAP). Chemical modulation was performed for the nitro-furan moiety, with changing the starting block from furan to thiophene or pyrrole *etc.* **2**–**8**. These compounds **2**–**8** were synthesized in the similar manner to compound **1**. The derivatives bearing 5-nitro-furan-2-ester scaffold, compounds **9**–**27**, were prepared by the reaction of converting 5-nitro-2-furoic acid into an acid chloride with thionyl chloride, followed by the nucleophilic substitution reaction in the presence of NEt_3 in tetrahydrofuran (THF) with setting the temperature at 0°C for the initial 30 min. and elevated it to r.t. afterward. Since a hydroxy group bound to phenyl ring is more reactive than a hydroxy group bound to alkane, the substitution reaction dominantly produced phenyl-ester linkage (**9**–**16**) when a nucleophilic reagent contained two hydroxy groups. When a nucleophilic reagent contained only one hydroxy group, the substitution reaction generated alkyl-ester linkage (**17**–**27**). Compounds **28**–**30** were produced by generating nitro-furan-carbonyl-alkyl-benzene through the reaction of Weinreb amides containing benzyl group with alkyl lithium, followed by incorporation of nitro group into the phenyl ring using white fuming nitric acid and acetic anhydride. Compounds **29** and **30** were separated by flash chromatography. Compounds **31**–**33** were generated by using hydroxy-amines as nucleophilic reagents.

Evaluation of Inhibitory Activity The 50% inhibitory concentration (IC_{50}) of the synthesized compounds for RT-associated RNase H activity was determined from the chemical concentration reducing the rate for substrate cleavage reaction to half relative to the control. A real-time monitoring assay was employed to estimate the IC_{50}.[21,22] In short, two oligo-nucleotides were annealed at final concentrations of 2.5 and 0.25 μM for substrate. One was oligo-ribonucleotide 5′-GAUCUGAGCCUGGGAGCU-3′ with 6-carboxy-fluorescein (FAM) conjugated at the 3′ end, and the other was oligo-deoxyribonucleotide 5′-AGCTCCCAGGCTCAGATC-3′ with black hole quencher (BHQ) conjugated at the 5′ end. Enzyme reaction with 100 ng RT, 0.025 μM oligo-ribonucleotide, and 0.25 μM oligo-deoxyribonucleotide was carried out in a volume of 10 μL at 37°C. Fluorescence at 488 nm was monitored every 150 s using a multimode detector.

HIV-1 RT was expressed in *Escherichia coli* and purified by using a HiTrap Ni affinity column. The purified RT was dialyzed to reduce the concentration of imidazole from the elution buffer and then incubated with human rino virus (HRV) 3C protease to cleave an N-terminal hexahistidine tag. The protein was further purified by nickel-coordinated nitrilotriacetic acid (Ni-NTA) to remove the uncleaved protein and HRV 3C protease. The RT was dialyzed against a buffer of 50 mM Tris–HCl at pH 7.5 and 200 mM NaCl and was stored at −20°C with adding 50% (v/v) glycerol.

Assessment of Cytotoxicity 3-(4,5-Dimethylthiazol-2-yl)-2,5-diphenyltetrazolium bromide (MTT) assay was carried out with 293T cell line. First, 100 μL medium (RPMI-1640) supplemented with 10% fetal bovine serum (FBS) containing 2% dimethylsulfoxide (DMSO) was loaded in a 96-well plate, and 200 μL medium with 10% FBS and 2% DMSO containing test compounds at a concentration of 200 μM was added to the wells in the first column of the plate. Different concentrations of compound were prepared for the second, third and fourth columns. The final concentrations of these columns were 100, 50, 25 and 12.5 μM, respectively. Second, 100 μL 293T cells at a concentration of 2×10^5/mL were added to the respective wells. The final concentration of DMSO in each well was 1%. Third, cells were incubated for 3 d at 37°C with 5% CO_2 atmosphere. A hundred micro liter of supernatant was removed from the cultured medium and 15 μL MTT reagent for dye solution was added to each well and the cells were incubated for 1 h. Then, 100 μL solution of stop mix was added, and the cells were incubated overnight at 4°C to sufficiently dissolve the dye. Finally, intensity of $OD_{570/690}$ was measured by a spectrofluorometer.

Molecular Dynamics Simulation A computational model of HIV-1 RT domain was constructed from an X-ray crystal structure with Protein Data Bank code 3QIO.[23] Atom coordinates for the missing residues were generated by using Modeller9.9.[24] According to the results of the recent X-ray crystallographic studies on the complex of RNase H domain and its inhibitors,[25–27] the RNase H domain contains two divalent metal ions at the center of the active site. Two Mn^{2+} ions in the crystal structure were replaced with Mg^{2+} ions. The protonation states of all of the ionazable residues were predicted by ProPKa program[28] in the presence of two Mg^{2+} ions at the active site. Atom charges of the compounds were determined from the electrostatic potential obtained from quantum chemical calculations, followed by the restrained electrostatic potential (RESP) fitting[29] in a similar manner to the previous studies.[30–33] The atom charge for Mg^{2+} ion was setting to 1.54, which was also determined by the RESP method based on the calculated electrostatic potential obtained by QM/MM technique carried out in a similar manner to the previous work.[20] An active compound was combined with HIV-1 RT domain, referring the binding structure predicted in our previous work.[20] The compound-bound RT model was placed in a rectangular box and solvated with TIP3P water molecules,[34] with all of the crystal water molecules remaining. Periodic boundary conditions were applied to avoid the edge effect in all calculations.

Minimizations and MD simulations were carried out using sander module of AMBER9.[35] The modified ff03 force field[36]

was used as the parameters for molecular dynamics. The cut-off distance for the long range electrostatic and van der Waals energy terms was set to 12.0 Å. The expansion and shrinkage of all covalent bonds connecting to hydrogen atom were constrained using the SHAKE algorithm.[37] Energy minimization was achieved in three steps. Initially, movement was allowed only for water molecules. Next, compound and divalent metal ions were allowed to move in addition to the water molecules. Finally, all atoms were allowed to move freely. In each step, energy minimization was executed by the steepest descent method for the first 10000 cycles and the conjugated gradient method for the subsequent 10000 cycles. After a 0.1 ns heating calculation until 310 K using the NVT ensemble condition, a 20 ns equilibrating calculation was executed at 1.0 atm and at 310 K under the NPT ensemble condition, with an integration time step of 2.0 fs.

Results

Eight analogues of 5-nitro-furan-2-carboxylic acid ester were synthesized by converting the 5-nitro-furan moiety into other functional groups and examined for their RNase H inhibitory activities (Table 1). Compound **1** has a typical chemical structure showing an inhibitory potency for HIV-1 RNase H enzymatic activity. This compound bears nitro-furan ester core connecting to the pentyl- and benzyl-bound amide group. Replacement of furan with thiophene largely decreased compound potency (**2**, **3**). Conversion of furan into pyrrole also resulted in complete loss of compound potency (**4**). Attaching a halogen to the 4th position of furan exhibited a slight increase of inhibitory activity (**5**), while a hydrophobic or aromatic substitute resulted in loss of inhibitory potency (**6**, **7**). Introduction of even a small hydrophobic group at the 3rd position of furan decreased inhibitory activity (**8**).

Table 1. RNase H Inhibitory Activity and Cytotoxicity of the Derivatives Modulated at Nitro-Furan Moiety

Compound	Structure	IC_{50} (μM)	CC_{50} (μM)
1	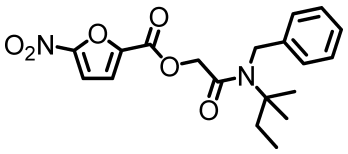	8.4	74
2	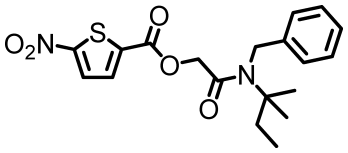	>50	49
3	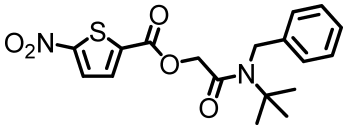	30.3	50
4	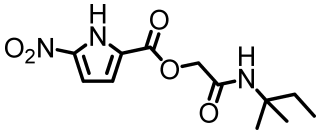	>50	86
5	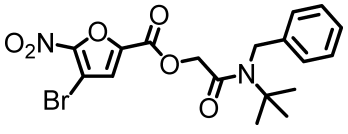	6.6	3
6	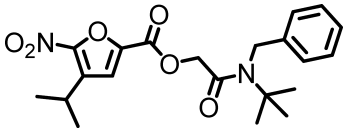	>50	>100
7	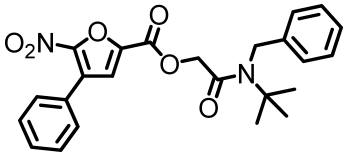	>50	>100
8	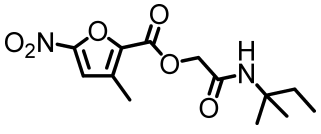	25.7	76

Eight derivatives bearing 5-nitro-furan phenyl ester core were examined as shown in Table 2. A similar degree of inhibitory activity was observed for the analogs having a hydroxy group at the *meta* or *para* position of phenyl ring (**9**–**11**). While substitution of the hydroxy group with acetyl group showed a similar degree of inhibitory activity (**12**), substitution with ethyl-ester increased compound potency (**13**). Further, introduction of methoxy group at the *ortho* position also increased compound potency (**14**). The compound containing methoxy-carbonyl and methoxy groups at the *para* or *ortho* positions exhibited a fine inhibitory activity (**15**). Introduction of phenyl-methyl-amine at the *para* position also maintained compound potency (**16**).

Eleven derivatives bearing 5-nitro-furan ester core bound with benzyl-based substitutes were investigated as summarized in Table 3. Connection of a benzyl group without any additional functional substitute showed moderate inhibitory activity (**17**). Attaching nitro group, methoxy-ether, or *tert*-butoxy-ester exhibited slight changes in compound potency (**18**–**20**). Extension of alkyl chain caused no significant difference in inhibitory potency (**21**). However, addition of hydroxy group decreased inhibitory activity (**22**). Introduction of methoxy group further decreased compound potency regardless of the position of the group bound to phenyl ring (**23**–**25**). While connection of two methoxy groups improved compound potency (**26**), replacement of two methoxy groups by chlorides showed low inhibitory activity (**27**).

Six derivatives were synthesized by changing the ester bond with carbonyl group as shown in Table 4. Ester linkage is disadvantageous for medicine because esterase digests the linkage and the drug concentration in a body decreases rapidly. Nitro-phenyl group was connected to the carbonyl carbon with changing the length of alkyl chain and the position of nitro group (**28**–**30**). None of the derivatives showed noticeable inhibitory activity. The ester linkage was replaced by an amide bond (**31**–**33**), in which hydroxy-methyl-benzyl, acetyl-methyl-benzyl, or bromo-methyl-benzyl was bound *via* a carbamoyl group. This modification also resulted in complete loss of compound potency.

Table 2. RNase H Inhibitory Activity and Cytotoxicity of the Derivatives Bearing Phenyl Ester Core

Compound	–O–R	IC_{50} (μM)	CC_{50} (μM)
9	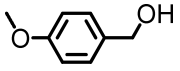	7.2	>100
10	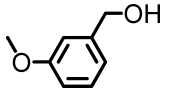	8.2	24
11	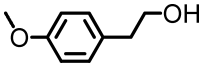	9.1	>100
12	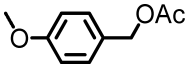	8.7	49
13	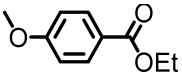	3.6	>100
14	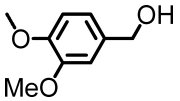	3.1	>100
15	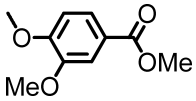	1.4	>100
16	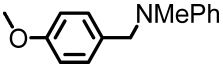	3.8	>100

Cytotoxicity was little or undetectable for most of the derivatives modulated at the nitro-furan moiety except for compound **5** (Table 1). No detectable cytotoxicity was also observed for most of the derivatives bearing nitro-furan-phenyl ester core (Table 2). It should be noted that highly active compounds, **14** and **15**, showed no noticeable cytotoxicity at a concentration of 100 μM. In contrast, the analogs bearing ester core bound with benzyl-based substitute showed some degree of cytotoxicity (Table 3). Further, the analogs converted the ester into amide or ketone showed cytotoxicity in which CC_{50} ranged from 9 to 32 μM (Table 4). Overall, in the measurement using 293T cells, half of the synthesized compounds showed noticeable cytotoxicity but almost all of the toxicity-detected compounds showed little RNase H inhibitory activity. Accordingly, the results of this assay suggest that active compounds have no significant cytotoxicity and the nitro-furan-phenyl ester skeleton is the most favorable among them from a cytotoxic viewpoint.

In order to examine the stability of the binding structure of a potent compound inside the active site of the target protein, MD simulation was performed for the complex of a synthesized derivative **15** and RNase H domain. MD simulation was carried out for 20 ns and root mean square deviation (RMSD) relative to the structure after heating was calculated as shown in Fig. S1 of the supplemental information. The RMSD value showed a gradual increase up to 5 ns and scarcely changed during later 15 ns. Accordingly, the binding conformation of the complex was judged to be equilibrated. In order to extract the snapshot structure representing a typical binding mode of compound **15** and RNase H domain, the averaged structure was obtained using 2500 trajectories from the last 5 ns of MD simulation. The RMSD between each trajectory and the average structure was calculated, and then one trajectory with the smallest RMSD value was determined to be the typical complex structure shown in Fig. 1a.

Two Mg^{2+} ions were held by the side chains of four acid residues; Asp443, Glu478, Asp498, Asp549, and the compound was stably bound to the active site without changing the binding mode during 20 ns simulation. In the binding structure, the nitro-furan-ester core is especially, stably bound to two Mg^{2+} ions as shown in Fig. 1a. A stereo view of the binding structure is presented in Fig. S2 of the supplemental information. The oxygen atom on the furan ring is oriented toward the divalent metals. Nitro oxygen and carbonyl oxygen of the ester are strongly coordinated to the respective Mg^{2+} ions. Therefore, a large ring-shaped configuration of –Mg–O–N–C–O–C–C–O–Mg– is formed. The inter-atomic distance between two Mg^{2+} ions is 3.8 Å. The distance between the nitro oxygen atom and one Mg^{2+} ion is 1.9 Å, and that between carbonyl oxygen and the other Mg^{2+} ion is also 1.9 Å. Figure

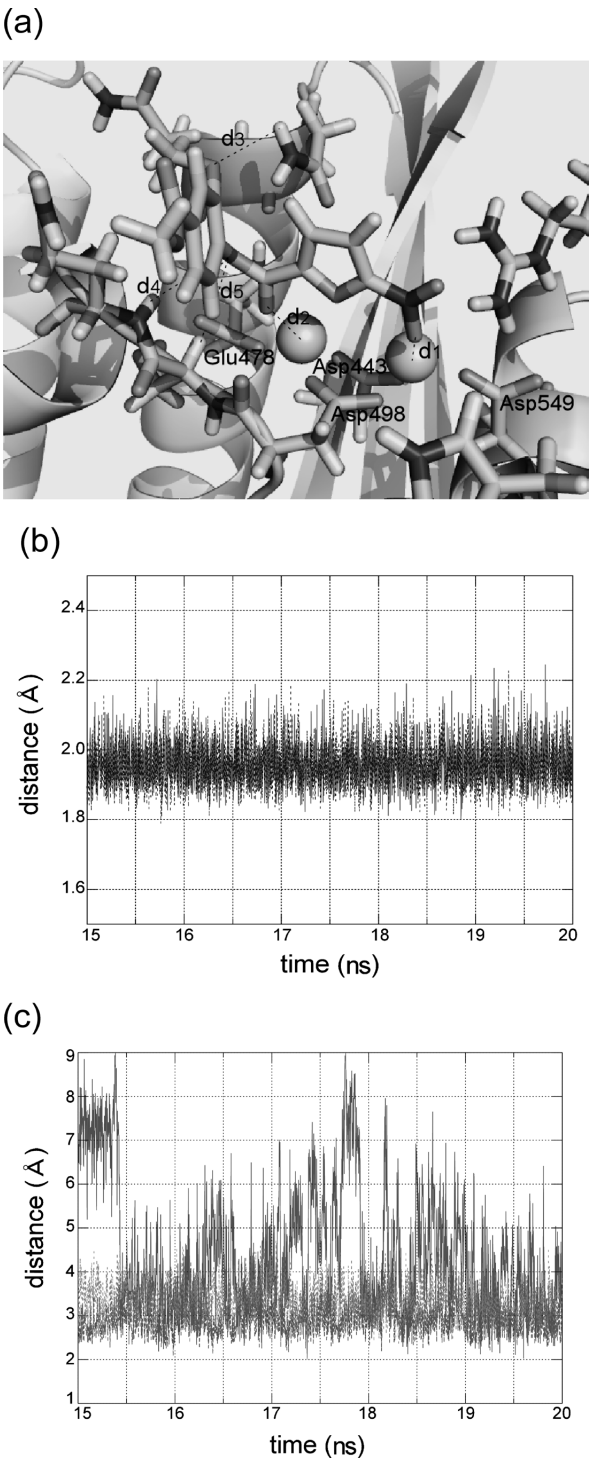

Fig. 1. (a) Binding Structure of an Active Compound to the RNase H Domain, Obtained by MD Simulation

Compound and several polar residues are shown in stick representation. Two Mg^{2+} ions are denoted by spheres. (b) Changes in the distances between nitro oxygen and Mg^{2+} ion (d_1: red solid line) and between carbonyl oxygen and another Mg^{2+} ion (d_2: blue dotted line) for the last 5 ns of MD simulation. (c) Changes in the distances between methoxy oxygen and amino hydrogen of Asn474 (d_3: green solid line), between ester oxygen and amide hydrogen of main chain of Gln500 (d_4: cyan broken line), and between ester oxygen and Cα hydrogen of Ser499 (d_5: yellow dotted line) for the last 5 ns of MD simulation. Color images were converted into gray scale; red solid line, blue dotted line, green solid line, cyan broken line, yellow dotted line have been converted into gray scale.

1b shows the changes of these two distances for the last 5 ns of MD simulation. These graphs clearly indicate that the interaction of oxygen atom and Mg^{2+} ion is quite strong and that the oxygen–Mg interaction is essentially important for the binding of potent compound.

Methoxy-carbonyl and methoxy groups connected to phenyl stick out from the binding pocket. The distance between methoxy oxygen and hydrogen atom of amino group of Asn474 was monitored as shown in Fig. 1c. The distance largely fluctuates during the simulation and the interaction is not so steady. Hence, there is much room for improvement in this region. The oxygen atom at the ester bond has noticeable interactions with the amide group of main chain of Gln500. The change of the distance between the ester oxygen and the hydrogen atom of the amide group is shown in Fig. 1c. No abrupt, large change is observed in the distance. Therefore, the interaction contributes to stabilizing the binding of the potent compound. The distance between the ester oxygen and the Cα hydrogen atom of Ser 499 was also monitored. The distance shows no large change for the last 5 ns of simulation, which suggests the stability of the binding of the ester part with RNase H domain. Consequently, it is confirmed from the MD simulation that an active compound **15** is stably bound to the active site of the RNase H domain with coordinating to two divalent metal ions and making supportive interaction at the ester part.

Discussion

According to the data summarized in Table 3, it is suggested that various kinds of functional groups connected to the benzyl ring have little interaction with the RNase H domain and that the functional group-binding region is located outside the binding pocket and is exposed to the solvent. Further, a comparison of inhibitory activity between compounds **17**–**20** and compounds **21**–**27** suggests that the length of alkyl chain connecting to phenyl ring has a significant influence on the difference in compound potency. That is, the longer alkyl chain in compounds **21**–**27** is less favorable in terms of both inhibitory activity and cytotoxicity. This indicates that a strategy to increase the inhibitory activity is to position the substitute closer to the nitro-furan group. The conversion may allow the aromatic ring or substitute to interact with the target protein inside the binding pocket.

A comparison of inhibitory activities of compounds in Tables 2 and 3 indicates that the introduction of phenyl-ester connected to nitro-furan shows higher compound potency than that of benzyl-ester. This is consistent with the findings described above paragraph and supports the notion that the compound potency increases when the position of the substitute connected to the ester linkage is closer to the nitro-furan. The incorporation of polarized substitutes like methoxy, hydroxy, methoxy-carbonyl, or ethoxy-carbonyl group is effective to increase the compound potency. In particular, the introduction of methoxy group at the *ortho*-position of phenyl ring effectively increases the inhibitory activity.

All the compounds in Tables 2 and 3 have the ester linkage. The data summarized in Table 4 clearly indicate that conversion of the ester linkage into carbonyl and/or amide bond results in loss of inhibitory potency. Both bonds will be likely to make the chemical to be in a straight configuration. If a compound has a straight form, the side part of the compound

Table 3. RNase H Inhibitory Activity and Cytotoxicity of the Derivatives Bearing Ester Core Bound with Benzyl-Based Substitute

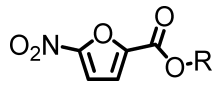

Compound	–O–R	IC_{50} (μM)	CC_{50} (μM)
17	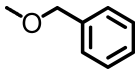	5.4	38
18	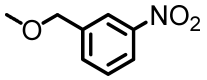	5.0	>100
19	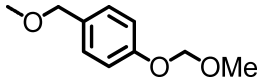	5.8	75
20	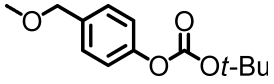	4.5	>100
21	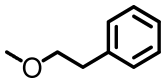	5.1	57
22	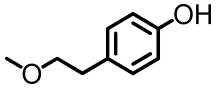	7.9	39
23	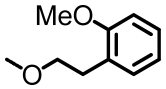	14.2	42
24	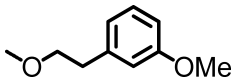	18.6	36
25	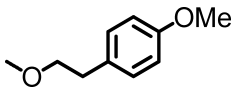	12.5	36
26	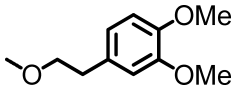	8.5	51
27	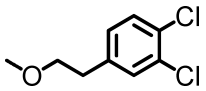	17.4	64

Table 4. RNase H Inhibitory Activity and Cytotoxicity of the Derivatives Converted the Ester Bond into Other Kinds of Linkages

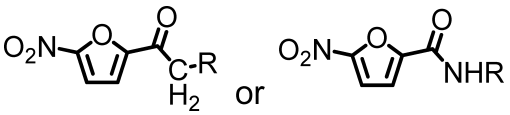

Compound	$–CH_2–R$ or –NH–R	IC_{50} (μM)	CC_{50} (μM)
28	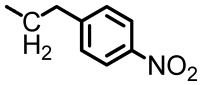	>50	11
29	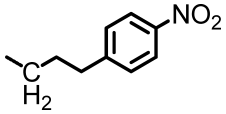	>50	17
30	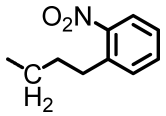	>50	9
31	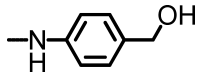	>50	29
32	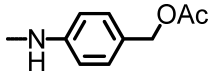	>50	27
33	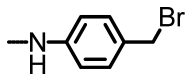	>50	32

will collide with the inside wall of the binding pocket of the RNase H domain. Accordingly, compounds are hardly combined with the binding pocket.

The conversion of the nitro-furan group into pyrrole drastically decreases the inhibitory activity while conversion to nitro-thiophen maintains the activity (Table 1). This indicates that a nitro-furan or nitro-thiophene core is indispensable for inhibitory potency. The characteristic property of nitro-furan is its large electric polarity. Oxygen atoms are negatively charged and these oxygen atoms will be coordinated to divalent metal ions at the RNase H active site. The attachment of non-polar substitute to furan results in decrease of compound potency. Accordingly, the 3rd and 4th positions of furan become close to the residues inside the RNase H active site.

RNase H of HIV-1 exerts its enzymatic activity by incorporating divalent metal ions at the reaction site.[38,39] It had been controversial how many metal ions were required at the RNase H reaction site to exert its enzymatic activity.[40] A theoretical study by De Vivo *et al.* suggested that the presence of two divalent metal ions is essential for RNase H activity and that two metal ions act cooperatively with facilitating the binding of a substrate and catalyzing the enzymatic reaction.[41] This theoretical finding strongly suggests double coordination of divalent metal ions at the RNase H domain. Crystal structures on the complex of the RNase H domain and its inhibitor were successively reported from three different research groups.[23,25–27] All of the crystal structures ever reported showed the presence of two metal ions at the active site. One of the divalent metal ions was held deep inside the binding pocket of the RT RNase H domain with making coordination bonds to three carboxyl groups of Asp443, Glu478 and Asp498. The other was fixed with making coordination bonds to two carboxyl groups of Asp443 and Asp549. The distance between two metal ions was about 4 Å. Every inhibitor in crystal structures was revealed to have a similar binding mode. That is, inhibitors are stabilized with forming coordination bonds to both metal ions. Accordingly, it is highly probable that the chemical compounds showing RNase H inhibitory activity examined in this study are also coordinated to two divalent metal ions. Hence, negatively charged oxygen atoms of the nitro group, furan, and carbonyl group are aligned in a straight form. This negatively charged region will be attached to the divalent metal ions.

The binding structure deduced from MD simulation indicates that ether oxygen at the ester bond has an interaction with a polar residue, Ser499, which is located at the deep inside of RNase H domain. This residue would have little

influence on the function of RNase H. Therefore, one of the designs to improve inhibitory activity is to modify the compound to bear some polar functional group that enables a strong interaction with Ser499. In order to enhance the binding affinity of the compounds with RNase H active site, the incorporation of a polar functional group bound to phenyl ring is one of the possible conversions of our derivatives. The distance between methoxy group and the amine of Asn474 largely fluctuated during MD simulation. If the interaction with Asn474 is enforced, compound will be more stably combined with the RNase H domain.

Conclusion

More than 30 chemical compounds were synthesized for developing the inhibitors of RNase H activity of HIV-1 reverse transcriptase. Inhibitory potency of RNase H enzymatic activity was measured in a biochemical assay with a real-time fluorescence monitoring method. The active compounds found in our previous studies commonly bear nitro-furan ring connecting to hydrophobic region *via* an ester linkage. Conversion of the nitro-furan group into pyrrole drastically decreased the inhibitory activity while conversion into nitro-thiophene maintained the compound potency. This means that the structural basis of nitro-furan or nitro-thiophene is indispensable for inhibitory activity. An improvement in compound potency was observed when a phenyl-ester moiety was connected to the nitro-furan and further methoxy-carbonyl and methoxy groups were bound to the phenyl ring. No notable change in inhibitory potency was observed when benzyl-ester based substitute was connected to nitro-furan. Modulation of ester linkage resulted in complete loss of compound potency. Molecular dynamics simulation was performed to examine the stability of the binding structure of a synthesized active compound to RNase H domain. It was demonstrated that a potent compound was stably bound to the active site with establishing strong coordinate bonds with divalent metal ions located at the active site. The present study provides important information for designing prospective chemical structures inhibiting HIV-1 RNase H activity.

Acknowledgments This work was supported by a Health and Labor Science Research Grant for Research on Publicly Essential Drugs and Medical Devices from the Ministry of Health and Labor of Japan. A part of this work was also supported by a Grant-in-Aid for Scientific Research (C) from Japan Society for the Promotion of Science (JSPS). Theoretical calculations were performed at the Research Center for Computational Science, Okazaki, Japan and at the Information Technology Center of the University of Tokyo and also by the high-performance computer system at Institute for Media Information Technology in Chiba University.

References

1) Goody R. S., Müller B., Restle T., *FEBS Lett.*, **291**, 1–5 (1991).
2) Ren J., Stammers D. K., *Virus Res.*, **134**, 157–170 (2008).
3) Andréola M. L., De Soultrait V. R., Fournier M., Parissi V., Desjobert C., Litvak S., *Expert Opin. Ther. Targets*, **6**, 433–446 (2002).
4) Klumpp K., Mirzadegan T., *Curr. Pharm. Des.*, **12**, 1909–1922 (2006).
5) Tramontano E., *Mini Rev. Med. Chem.*, **6**, 727–737 (2006).
6) Tanese N., Telesnitsky A., Goff S. P., *J. Virol.*, **65**, 4387–4397 (1991).
7) Telesnitsky A., Goff S. P., *EMBO J.*, **12**, 4433–4438 (1993).
8) Borkow G., Fletcher R. S., Barnard J., Arion D., Motakis D., Dmitrienko G. I., Parniak M. A., *Biochemistry*, **36**, 3179–3185 (1997).
9) Tramontano E., Esposito F., Badas R., Di Santo R., Costi R., La Colla P., *Antiviral Res.*, **65**, 117–124 (2005).
10) Tarrago-Litvak L., Andreola M. L., Fournier M., Nevinsky G. A., Parissi V., de Soultrait V. R., Litvak S., *Curr. Pharm. Des.*, **8**, 595–614 (2002).
11) Cowan J. A., Ohyama T., Howard K., Rausch J. W., Cowan S. M., Le Grice S. F., *J. Biol. Inorg. Chem.*, **5**, 67–74 (2000).
12) Haren L., Ton-Hoang B., Chandler M., *Annu. Rev. Microbiol.*, **53**, 245–281 (1999).
13) Steitz T. A., Smerdon S. J., Jäger J., Joyce C. M., *Science*, **266**, 2022–2025 (1994).
14) Nowotny M., Gaidamakov S. A., Crouch R. J., Yang W., *Cell*, **121**, 1005–1016 (2005).
15) Nowotny M., Gaidamakov S. A., Crouch R. J., Yang W., *EMBO J.*, **25**, 1924–1933 (2006).
16) Shaw-Reid C. A., Munshi V., Graham P., Wolfe A., Witmer M., Danzeisen R., Olsen D. B., Carroll S. S., Embrey M., Wai J. S., Miller M. D., Cole J. L., Hazuda D. J., *J. Biochem.*, **278**, 2777–2780 (2003).
17) Hang J. Q., Rajendran S., Yang Y., Li Y., In P. W. K., Overton H., Parkes K. E. B., Cammack N., Martin J. A., Klumpp K., *Biochem. Biophys. Res. Commun.*, **317**, 321–329 (2004).
18) Budihas S. R., Gorshkova I., Gaidamakov S., Wamiru A., Bona M. K., Parniak M. A., Crouch R. J., McMahon J. B., Beutler J. A., Le Grice S. F., *Nucleic Acids Res.*, **33**, 1249–1256 (2005).
19) Fuji H., Urano E., Futahashi Y., Hamatake M., Tatsumi J., Hoshino T., Morikawa Y., Yamamoto N., Komano J., *J. Med. Chem.*, **52**, 1380–1387 (2009).
20) Yanagita H., Urano E., Matsumoto K., Ichikawa R., Takaesu Y., Ogata M., Murakami T., Wu H. G., Chiba J., Komano J., Hoshino T., *Bioorg. Med. Chem.*, **19**, 816–825 (2011).
21) Chan K. C., Budihas S. R., Le Grice S. F., Parniak M. A., Crouch R. J., Gaidamakov S. A., Isaaq H. J., Wamiru A., McMahon J. B., Beutler J. A., *Anal. Biochem.*, **331**, 296–302 (2004).
22) Parniak M. A., Min K. L., Budihas S. R., Le Grice S. F., Beutler J. A., *Anal. Biochem.*, **322**, 33–39 (2003).
23) Lansdon E. B., Liu Q., Leavitt S. A., Balakrishnan M., Perry J. K., Lancaster-Moyer C., Kutty N., Liu X., Squires N. H., Watkins W. J., Kirschberg T. A., *Antimicrob. Agents Chemother.*, **55**, 2905–2915 (2011).
24) Martí-Renom M. A., Stuart A. C., Fiser A., Sánchez R., Melo F., Sali A., *Annu. Rev. Biophys. Biomol. Struct.*, **29**, 291–325 (2000).
25) Kirschberg T. A., Balakrishnan M., Squires N. H., Barnes T., Brendza K. M., Chen X., Eisenberg E. J., Jin W., Kutty N., Leavitt S., Liclican A., Liu Q., Liu X., Mak J., Perry J. K., Wang M., Watkins W. J., Lansdon E. B., *J. Med. Chem.*, **52**, 5781–5784 (2009).
26) Himmel D. M., Maegley K. A., Pauly T. A., Bauman J. D., Das K., Dharia C., Clark A. D. Jr., Ryan K., Hickey M. J., Love R. A., Hughes S. H., Bergqvist S., Arnold E., *Structure*, **17**, 1625–1635 (2009).
27) Su H. P., Yan Y., Prasad G. S., Smith R. F., Daniels C. L., Abeywickrema P. D., Reid J. C., Loughran H. M., Kornienko M., Sharma S., Grobler J. A., Xu B., Sardana V., Allison T. J., Williams P. D., Darke P. L., Hazuda D. J., Munshi S., *J. Virol.*, **84**, 7625–7633 (2010).
28) Li H., Robertson A. D., Jensen J. H., *Proteins*, **61**, 704–721 (2005).
29) Cieplak P., Cornell W. D., Bayly C., Kollman P. A., *J. Comput. Chem.*, **16**, 1357–1377 (1995).
30) Matsuyama S., Aydan A., Ode H., Hata M., Sugiura W., Hoshino T., *J. Phys. Chem. B*, **114**, 521–530 (2010).
31) Sano E., Li W., Yuki H., Liu X., Furihata T., Kobayashi K., Chiba K., Neya S., Hoshino T., *J. Comput. Chem.*, **31**, 2746–2758 (2010).

32) Ode H., Neya S., Hata M., Sugiura W., Hoshino T., *J. Am. Chem. Soc.*, **128**, 7887–7895 (2006).
33) Ode H., Matsuyama S., Hata M., Neya S., Kakizawa J., Sugiura W., Hoshino T., *J. Mol. Biol.*, **370**, 598–607 (2007).
34) Jorgensen W. L., Chandrasekhar J., Madura J. D., Impey R. W., Klein M. L., *J. Chem. Phys.*, **79**, 926–935 (1983).
35) Case D. A., Darden T. A., Cheatham T. E. III, Simmerling C. L., Wang J., Duke R. E., Luo R., Merz K. M., Pearlman D. A., Crowley M., Walker R. C., Zhang W., Wang B., Hayik S., Roitberg A., Seabra G., Wong K. F., Paesani F., Wu X., Brozell S., Tsui V., Gohlke H., Yang L., Tan C., Mongan J., Hornak V., Cui G., Beroza P., Mathews D. H., Schafmeister C., Ross W. S., Kollman P. A., "AMBER 9," University of California, San Francisco, 2006.
36) Katagiri D., Fuji H., Neya S., Hoshino T., *J. Comput. Chem.*, **29**, 1930–1944 (2008).
37) Ryckaert J.-P., Ciccotti G., Berendsen H. J. C., *J. Comput. Phys.*, **23**, 327–341 (1977).
38) Sarafianos S. G., Das K., Tantillo C., Clark A. D. Jr., Ding J., Whitcomb J. M., Boyer P. L., Hughes S. H., Arnold E., *EMBO J.*, **20**, 1449–1461 (2001).
39) Huang H., Chopra R., Verdine G. L., Harrison S. C., *Science*, **282**, 1669–1675 (1998).
40) Klumpp K., Hang J. Q., Rajendran S., Yang Y., Derosier A., Wong Kai In P., Overton H., Parkes K. E., Cammack N., Martin J. A., *Nucleic Acids Res.*, **31**, 6852–6859 (2003).
41) De Vivo M., Dal Peraro M., Klein M. L., *J. Am. Chem. Soc.*, **130**, 10955–10962 (2008).